acta physica slovaca vol. 54 No. 2, 191 – 204 **April 2004**

THE STUDY OF THE (n,2n) REACTION CROSS-SECTIONS FOR NEIGHBOR DEFORMED NUCLEI IN THE REGION OF RARE-EARTH ELEMENTS

E. Tel*, Ş. Okuducu†[1], A. Aydin‡, B. Şarer* , G. Tanir*

* *Gazi University, Faculty of Arts and Science, 06500 Ankara, Turkey*

† *Gaziosmanpaşa University, Faculty of Arts and Science, 60250 Tokat, Turkey*

‡ *Kirikkale University, Faculty of Arts and Science, 71400 Kirikkale, Turkey*

Received 22 July 2003 in final form 31 January 2004, accepted 10 February 2004

The (n,2n) reaction cross-section calculations for some neighbor deformed target nuclei have been made in the region of rare-earth elements between 8 and 24 MeV incident energy. In the calculations, the geometry dependent hybrid model and the exciton model have been used including the effects of pre-equilibrium. Pre-equilibrium direct effects have been examined using full exciton model. The measured cross-sections are taken from literatures. The cross-sections were calculated using other semi-empirical formulas for the incoming energieswhich satisfy the condition $U_{\mathrm{R}} = E_{\mathrm{n}} + Q_{\mathrm{n,2n}} = 6 \pm 1$ MeV. The obtained results were discussed and compared with the available experimental data, and found to be well in agreement.

PACS: 27.70.+q , 24.10.-I

1 Introduction

Applications of statistical and thermodynamical methods for heavy nuclei go back to the fundamental works of Bohr [1] and Frenkel [2]. Bohr suggested that collision of fast neutrons with heavy nuclei leads to the formation of compound systems, which are characterized with relative stability. Due to the dense packing of nucleons the energy exchange between the nuclear particles becomes essential. Frenkel put the idea of neutron evaporation forward for the calculation of neutron emission probability from a compound nucleus. Further, the knowledge of (n,2n) cross-section is quite essential in the reactor technology as a significant portion of the fission neutron spectrum which lies above the threshold of (n,2n) reaction for most of the reactor materials. It has been established that pre-equilibrium processes play an important role in nuclear reactions induced by light projectiles with incident energies above about 10 MeV. Starting with the introduction of exciton model [3] by Griffin in 1966, a series of semi classical models [4,5] of varying complexities have been developed for calculating and evaluating particle emissions in the continuum. It was also shown that with some freedom in the choice of parameters, these models could give reasonable fit to the observed energy and angular distributions of the emitted particles. More recently, researchers have formulated several quantum–mechanical reaction

[1]E-mail address: okuducu@gop.edu.tr

theories [6,7] that are based on multi-step concepts and in which statistical evaporation at lower energies is connected to direct reactions at higher energies.

The character of the nuclear deformation can be seen in the mass regions $150 < A < 190$ and $A > 220$, which correspond respectively to the rare-earth and actinide elements. In these regions, the energies of the first excited states are smaller than those of other nuclei and they have large values of quadrupole moments as such nuclei are far away from closed-shell configurations [8,9]. The knowledge of these cross-sections should be useful for studying the accuracy of the statistical model in describing the (n,2n) reactions on nuclei which are deformed and/or lie off the stability line. In present paper, by using equilibrium and pre-equilibrium reaction mechanisms, the (n,2n) cross-section values for some neighbor deformed target nuclei between 8 and 24 MeV incident energy in the region of rare-earth elements have been calculated and compared with the experimental results.

2 Exciton model

Equilibrium emission is calculated according to Weisskopf-Ewing (WE) model [10] by neglecting angular momentum. In the evaporation, the basic parameters are binding energies, inverse reaction cross-section, the pairing and the level-density parameters. The reaction cross-section for the incident channel a and exit channel b can be written as

$$\sigma_{ab}^{\mathrm{WE}} = \sigma_{ab}(E_{\mathrm{inc}}) \frac{\Gamma_b}{\sum\limits_{b'} \Gamma_{b'}}, \tag{1}$$

where E_{inc} is the incident energy. In Eq. (1), Γ_b can be also expressed as

$$\Gamma_b = \frac{2s_b + 1}{\pi^2 \hbar^2} \mu_b \int \mathrm{d}\varepsilon \sigma_b^{\mathrm{inv}}(\varepsilon) \varepsilon \frac{\omega_1(U)}{\omega_1(E)},$$

where U, μ_b, s_b, σ_b^{inv} are the excitation energy of the residual nucleus, the reduced mass, the spin, and the inverse reaction cross-section, respectively. The total single-particle level density is taken as,

$$\omega_1(E) = \frac{1}{\sqrt{48}} \frac{\exp\left[2\sqrt{\alpha(E-D)}\right]}{E-D}; \qquad \alpha = \frac{6}{\pi^2} g, \tag{2}$$

where E, D, and g are the excitation energy of the compound nucleus, the pairing energy, and the single particle level density, respectively.

The exciton model uses a unified model based on the solution of the master equation [11] in the form proposed by Cline [12] and Ribansky et al. [13]. Integrating the master equation over time,

$$\begin{aligned} -q(n, t=0) \quad &= \lambda^+(E, n+2)\tau(n+2) + \lambda^-(E, n-2)\tau(n-2) \\ &- \left[\lambda^+(E, n) + \lambda^-(E, n) + W_\lambda(E, n)\right] \tau(n), \end{aligned} \tag{3}$$

where $q(n, t = 0)$ is the initial condition on the process. $\tau(n)$ is the solution of the master equation which represents the time during which the system remains in a state of n excitons. The $\lambda^+(E, n)$ and $\lambda^-(E, n)$ are the internal transition rates and the use of master equation (3),

which includes both the probabilities of transition to equilibrium $\lambda^+(E,n)$ and probabilities of return to less complex stage $\lambda^-(E,n)$. $W_\lambda(E,n)$ is the emission rate for a state with an n-exciton configuration. Expressions formally identical to the conventional Weisskopf 's ones for the evaporation from the compound nucleus are thus obtained, with the only difference deriving from the introduction of the densities of particle (p) and hole (h) states. In order to solve the system of algebraic equations (3), it was used the algorithm proposed by Akkermans et al. [14], which gives an accurate result for any initial condition of the problem.

The methods proposed by Cline [11,12] and Kalbach [15] were used to calculate the probability of nucleon emission. They obtained the expressions for emission probability applying the principle of detailed balance in a way similar to that in the evaporation model. The probability of emission $W_b(E,n,\varepsilon_b)$ of a nucleon b with energy ε_b from a state with p excited particles and h holes (n excitons) is given by

$$W_b(E,n,\varepsilon_b) = \frac{2s_b+1}{\pi^2\hbar^3}\varepsilon_b\mu_b\sigma_b^{\mathrm{inv}}(\varepsilon_b)\frac{\omega(p-p_b,h,U)}{\omega(p,h,E)}Q_b(p,h), \tag{4}$$

where factor $Q_b(p,h)$, which takes into account the difference between neutrons and protons, can be used in the Kalbach Form [15] or as proposed by Gupta [16]. In both cases it is guaranteed that if $n > n_{eq}$ then $Q_b(p,h) \equiv 1$. Moreover, both factors are equal if quantity of neutrons in the compound nucleus is equal to that of protons. The results obtained show that the relative importance of using factor Q increases with the mass number and that it is decisive in the case of medium and heavy nuclei, where the neutron-proton difference is appreciable [16].

It is well known that during nucleon scattering in the vibrational nuclei there occur processes of direct excitation of low excitation energy levels of collective type. At the latest specialists' meetings on nuclear data calculation it was pointed out that a correct description of the high-energy emission spectrum in neutron-induced reactions could be obtained only if direct processes were taken into account. The experimental evidence in support of this type of mechanism has been confirmed by the latest experiment with the (n,n') reactions with a very good resolution [17,18]. In the experimental spectra, we can clearly see a structure of peaks which corresponds to the excitations of the direct type. The parametrization was adopted in Ref. [19] to describe this phenomenon. In accordance with this parametrization, the differential cross-section of neutron emission by the direct interaction in the (n,n') reaction can be written as,

$$\frac{\mathrm{d}\sigma_{ab}^{\mathrm{dir}}}{\mathrm{d}\varepsilon_b}(\varepsilon_b) = \left[\frac{2\mu}{\hbar^2}\right]\frac{V}{(k_aR)^2}\frac{k_b}{k_a}P_a(\varepsilon_a)P_b(\varepsilon_b)V_R^2\sum_{\lambda=2}^{3}\frac{\beta_\lambda^2}{(2\lambda+1)}\delta(U-\omega_\lambda), \tag{5}$$

where V, R, V_R are the volume of the nuclei, the radius of nuclei, and the potential well depth taken to be 48 MeV, respectively. $P_a(\varepsilon_a) = 4k_aK_a/(k_a+K_a)$ is the coefficient of the penetrability, k_a and K_a being particle momenta inside and outside the nucleus. β_λ and ω_λ are deformation and energy parameters which correspond to the target nucleus levels of the collective type. Only the octupolar and quadrupolar oscillations are considered. The ω_2, β_2 values for even nuclei were taken from Ref. [20]. In the case of odd nuclei, on the assumption of a weak bond, the values corresponding to the neighbouring even nucleus are used. The ω_3 value was taken from Ref. [21]. The octupolar deformation parameters were calculated from $\beta_3^2 = (2\lambda+1)\omega_3$ [MeV]/1000. Capote et al. have replaced the function $\delta(U-\omega_\lambda)$, which

relates the excitation energy of the residual nucleus to the energy the collective state and to emission energy, by Gaussian whose semi-width is chosen to taking into account the experimental energy resolution. The parametrization used in Eq. (5) assumes the superficial nature of the direct interaction.

3 Geometry Dependent Hybrid Model

The hybrid model for pre-compound decay is given by Blann and Vonach [22] as

$$\frac{\mathrm{d}\sigma_{\upsilon}(\varepsilon)}{\mathrm{d}\varepsilon} = \sigma_R P_{\upsilon}(\varepsilon), \tag{6}$$

and

$$P_{\upsilon}(\varepsilon)\mathrm{d}\varepsilon = \sum_{\substack{n=n_0 \\ \Delta n=+2}}^{\bar{n}} \left[{}_n\chi_{\upsilon} N_n(\varepsilon, U)/N_n(E)\right] g\mathrm{d}\varepsilon \left[\lambda_c(\varepsilon)/(\lambda_c(\varepsilon) + \lambda_+(\varepsilon)\right] D_n, \tag{7}$$

where σ_R is the reaction cross-section, ${}_n\chi_{\nu}$ is the number of particle type ν (proton or neutron) in n exciton hierarchy, $P_{\upsilon}(\varepsilon)\mathrm{d}\varepsilon$ represents number of particles of the ν (neutron or proton) emitted into the unbound continuum with channel energy between ε and $\varepsilon + \mathrm{d}\varepsilon$. The quantity in the first set of square brackets of Eq. (7) represents the number of particles to be found (per MeV) at a given energy ε for all scattering processes leading to an "n" exciton configuration. $\lambda_c(\varepsilon)$ is emission rate of a particle into the continuum with channel energy ε and $\lambda_+(\varepsilon)$ is the intranuclear transition rate of a particle. It has been demonstrated that the nucleon-nucleon scattering energy partition function $N_n(E)$ is identical to the exciton state density $\rho_n(E)$, and may be derived by the certain conditions on N-N (nucleon-nucleon) scattering cross-sections [23]. The second set of square brackets in Eq. (7) represents the fraction of the ν type particles at a energy which should undergo emission into the continuum, rather than making an intranuclear transition. The D_n represents the average fraction of the initial populatin surviving to the exciton number being treated.

Early comparisons among experimental results, pre-compound exciton model calculations, and intranuclear cascade calculations indicated that the exciton model gave too few pre-compound particles and that these were too soft in spectral distribution for the expected initial exciton configurations. The intranuclear cascade calculations results indicated that the exciton model deficiency resulted from a failure to properly reproduce enhanced emission from the nuclear surface [22].

In order to provide a first order correction for this deficiency the hybrid model was reformulated by Blann and Vonach. In this way the diffuse surface properties sampled by the higher impact parameters were crudely incorporated into the pre-compound decay formalism, in the geometry dependent hybrid model (GDH). The differential emission spectrum is given in the GDH as

$$\frac{\mathrm{d}\sigma_{\upsilon}(\varepsilon)}{\mathrm{d}\varepsilon} = \pi\lambda\!\!\!^{-2} \sum_{l=0}^{\infty} (2l+1) T_l P_{\upsilon}(l, \varepsilon), \tag{8}$$

where $\lambda\!\!\!^{-}$ is the reduced de Broglie wavelength of the projectile and T_l represents transmission coefficient for l^{th} partial wave. Using the total pre-compound neutron emission spectrum

$\mathrm{d}\sigma_n(\varepsilon)/\mathrm{d}\varepsilon$, the cross-section which could be involved in the emission of two neutrons is calculated as

$$\sigma_{2n} = \int_{U=0}^{E-B_{2n}} \frac{\mathrm{d}\sigma_n(\varepsilon)}{\mathrm{d}\varepsilon}\mathrm{d}\varepsilon,$$

where B_{2n} represents the sum of the first and the second neutron binding energies.

The geometry dependent influences are manifested in two distinct manners in the formulation of the GDH model. The more obvious is the longer mean free path predicted for nucleons in the diffuse surface region. The second effect is less physically secure, yet seems to be important in reproducing experimental spectral shapes. The nuclear density distribution used in the GDH model is a Fermi density distribution function, $\rho(R_l) = \rho_s \left[\exp(R_l - C)/0.55\ fm + 1\right]^{-1}$, where ρ_s is the density at the center of nucleus, and $C = 1.07A^{1/3}$ fm taken from electron scattering results [24]. The radius for the l^{th} entrance channel partial was defined by $R_l = \lambda\!\!\!^{-}(l + 1/2)$. In the GDH model, the fermi energies and nuclear densities are defined to impact parameter R_l.

4 Semi-empirical formulas for (n,2n) reaction cross-section

Q-value plays an important role on (n,2n) cross-sections at given incident neutron energy E_n. However, it is essential to look for the dependence of (n,2n) cross-sections on the asymmetry parameter at a given maximal residual excitation energy, $U_{\mathrm{R}} = E_{\mathrm{n}} + Q_{\mathrm{n,2n}} = 6 \pm 1$ MeV. The (n,2n) reaction has been frequently investigated in the past. Until now a large number of experimental data have been published on the (n,2n) reaction cross-sections induced by 14 to 15 MeV neutrons (see, for example, the Computer index of Neutron Data bibliographic catalogue). Most of the experimental data are taken at energies near 14 MeV neutron energy. There are several formulas describing the isotopic dependence of cross-sections for different reactions at neutron energy of 14.5 MeV. The measured cross-sections exhibit a large gradient for the lighter masses ($Z \leq 30$) with increasing asymmetry parameter and then become almost constant for medium and heavy mass nuclei (starting from $A \leq 100$) [25]. Recently and many years ago the various attempts [26-29] were made to describe the compiled experimental values by formula relating the neutron-induced cross-sections to the $s = (N - Z)/A$ asymmetry parameter.

Konno et al. [27] have suggested a phenomenological formula for 14.9 MeV neutrons (in mb) as follows:

$$\ln(\sigma_{\mathrm{n,2n}}) = 7.434\left[1 - 1.484\exp(-27.37\ s)\right]. \tag{9}$$

Figure 1 shows the ratio of experimental to the calculated (n,2n) cross-sections for the incident energies E_n for the condition $U_{\mathrm{R}} = E_{\mathrm{n}} + Q_{\mathrm{n,2n}} = 6 \pm 1$ MeV, where U_{R} is the excitation energy of the residual nucleus. The experimental values are about 10-20% higher than calculated (n,2n) cross-sections for this formula. Q-values were taken from Ref. [30].

Bychkov et al. [28] have formulated for (n,2n) cross-sections as given by

$$\sigma_{\mathrm{n,2n}} = \begin{cases} 1000 + 7.5A(7.8s - 0.234) & \text{if} \quad s \leq 0.13, \\ 1000 + 7.5A(0.65 + s) & \text{if} \quad s > 0.13. \end{cases} \tag{10}$$

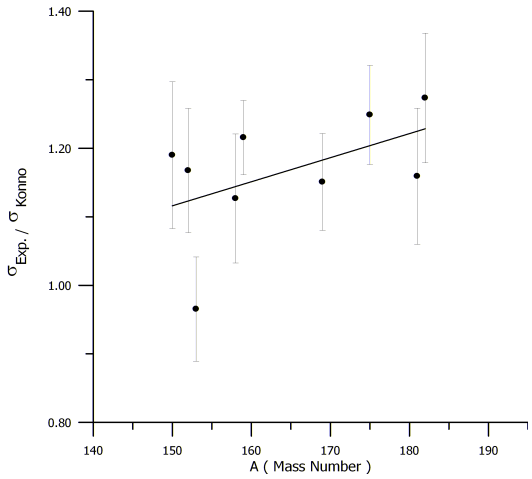

Fig. 1. The ratios of experimental (n,2n) cross-sections to the present compound-nucleus calculations versus the atomic mass number of the target nuclei, for $U_{\rm R} = 6 \pm 1$ MeV. The full line represents the linear function $y(A) = \sigma_{\rm exp.}/\sigma_{\rm calc.} = 0.00351098A + 0.59$, obtained by least-squares fit to the data. The experimental data were taken from Refs. [38-43].

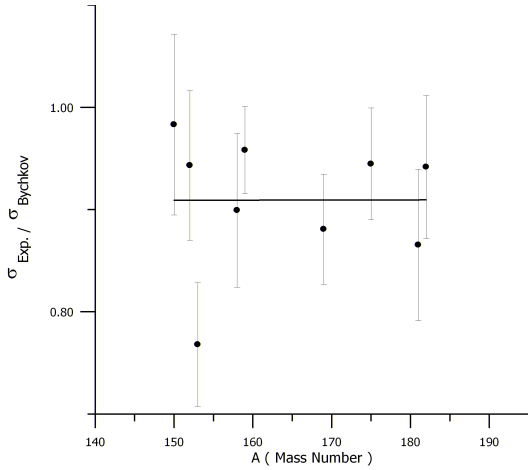

Fig. 2. The ratios of experimental (n,2n) cross-sections to the present compound-nucleus calculations versus the atomic mass number of the target nuclei, for $U_{\rm R} = 6 \pm 1$ MeV. The full line represents the linear function $y(A) = \sigma_{\rm exp.}/\sigma_{\rm calc.} = 0.00000099A + 0.90$, obtained by least-squares fit to the data. The experimental data were taken from Refs. [38-43].

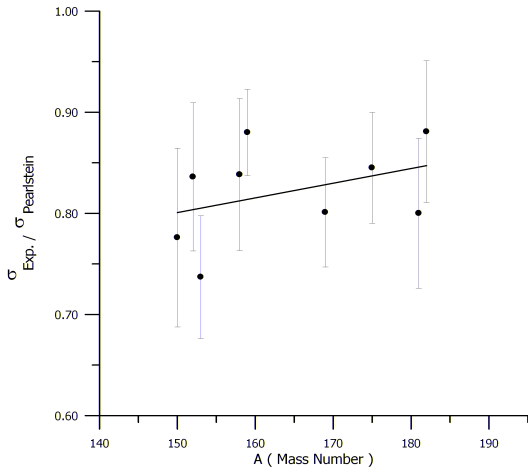

Fig. 3. The ratios of experimental (n,2n) cross-sections to the present compound-nucleus calculations versus the atomic mass number of the target nuclei, for $U_{\rm R} = 6 \pm 1$ MeV. The full line represents the linear function $y(A) = \sigma_{\rm exp.}/\sigma_{\rm calc.} = 0.0014509A + 0.58$, obtained by least-squares fit to the data. The experimental data were taken from Refs. [38-43].

Figure 2 shows the ratio of experimental to the calculated (n,2n) cross-sections. Although the experimental values are about 5-10% lower than the calculated, there is a good agreement between the calculated and measured (n,2n) data.

The (n,2n) reaction cross-sections were also studied by Pearlstein [29] using the following formula,

$$\sigma_{\rm n,2n}(E) = \sigma_{ne} \frac{\sigma_{n,M}}{\sigma_{ne}} \frac{\sigma_{\rm n,2n}(E_{\rm inc})}{\sigma_{n,M}}, \tag{11}$$

where $E_{\rm inc}$ is the incident neutron energy and σ_{ne} nonelastic cross-section. The sum of the (n,n'), (n,2n), (n,3n), etc. cross-sections belonging to this class is given the symbol $\sigma_{n,M}$. Figure 3 shows the ratio of experimental to the calculated (n,2n) cross-sections. The experimental values are about 10-20% lower than the calculated (n,2n) cross-sections.

5 Results and discussion

In this study, (n,2n) reaction cross-sections for ^{150}Nd, ^{152}Sm, ^{153}Eu, ^{158}Gd, ^{159}Tb, ^{169}Tm, ^{175}Lu, ^{181}Ta, and ^{182}W were calculated using equilibrium and pre-equilibrium reaction mechanisms. The equilibrium calculations were made by using Weisskopf-Ewing (WE) model. Exciton model and geometry depended hybrid model were used for pre-equilibrium calculations. The calculations have been made in the framework of the GDH model using ALICE/LIVERMORE-82 computer code [31]. The other theoretical calculations have also been made in the framework of the exciton model using PCROSS computer code [19]. The calculated excitation functions

have been obtained on the basis of the exciton model and geometry dependent hybrid model. In Figs. 4 to 12, the calculated (n,2n) cross-sections values have been compared with the experimental values.

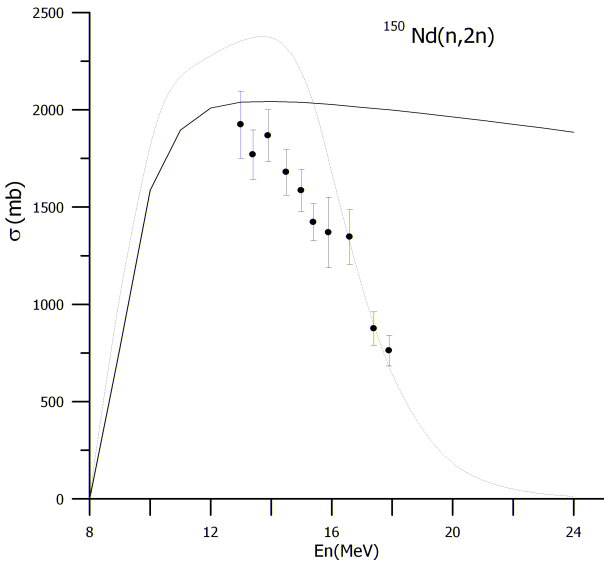

Fig. 4. The calculated and experimental (n,2n) cross-section for ^{150}Nd(n,2n). The solid curve is exciton model plus evaporation; the dashed curve is GDH model plus evaporation. The experimental data were taken from Ref. [38].

In calculations of the exciton model, PCROSS program code uses the initial exciton number as $n_0 = 1$, thus taking into account the direct gamma emission. Equilibrium exciton number is taken as $\sqrt{1.4\,gE}$ suggested by Williams [32], after Pauli correction was modified. Single particle level density parameter g was equal to $A/13$ in the exciton model calculation, where A is the mass number. Level density expression given by Dilg [33] was used in the evaporation model calculation. Particle-hole state density expression reported by Williams was used in the pre-equilibrium model calculation. The reaction cross-sections and the inverse cross-sections were obtained using the optical potential parameters by Wilmore and Hodgson [34], Bechetti and Greenlees [35], Huizenga and Igo [36] for neutrons, protons and alpha particles, respectively.

In calculations of the GDH model, ALICE/LIVERMORE-82 code uses the initial exciton number as $n_0 = 3$. In this model, it is used the initial neutron (n) and proton (p) exciton numbers in the calculations for neutron induced reactions. These exciton numbers are given by Blann and Vonach [22] as, ${}_3X_n = 2(3Z + 2N)/(3Z + 2N + 3Z)$ and ${}_3X_p = 2 - {}_3X_n$. N and Z are the neuron and proton numbers of the target nuclei, respectively. The standard pairing shift (zero for odd-even nuclei, delta for odd-odd nuclei) proposed by Blann and Bisplinghoff [31] was employed as the pairing correction for GDH model calculation. In the GDH model, the level density expression using the formula with mass shell corrections was used for ^{150}Nd, ^{152}Sm, ^{153}Eu, ^{158}Gd, ^{159}Tb, ^{169}Tm, and ^{175}Lu. The Fermi-gas level density expression was used for ^{181}Ta and ^{182}W.

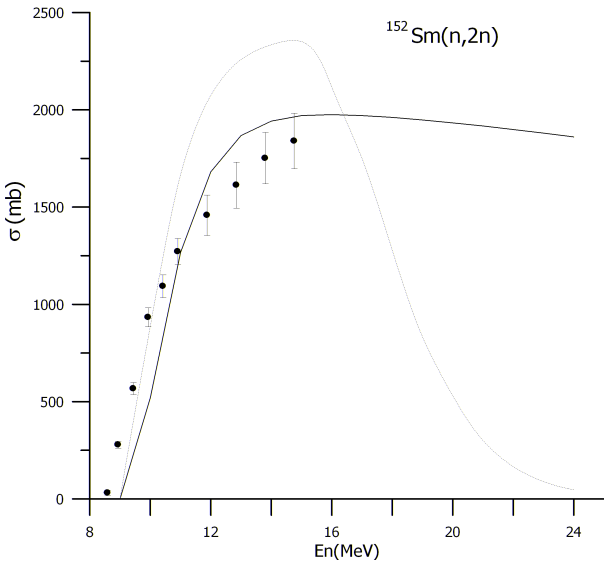

Fig. 5. The calculated and experimental (n,2n) cross-section for ^{152}Sm(n,2n). The solid curve is exciton model plus evaporation; the dashed curve is GDH model plus evaporation. The experimental data were taken from Ref. [39].

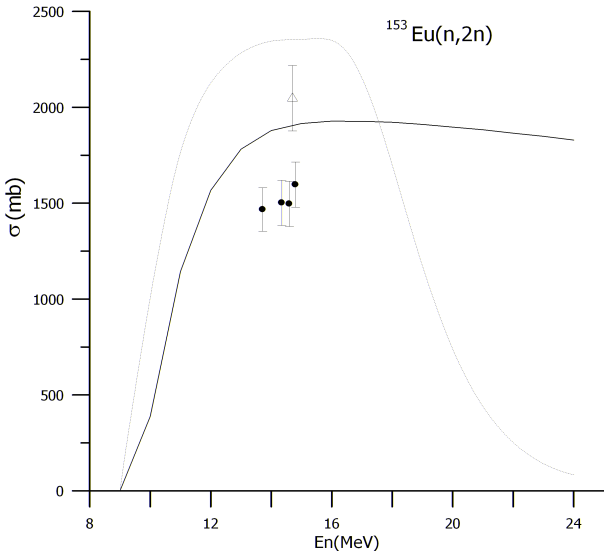

Fig. 6. The calculated and experimental (n,2n) cross-section for ^{153}Eu(n,2n). The solid curve is exciton model plus evaporation; the dashed curve is GDH model plus evaporation. The triangle symbols were taken from Ref. [41] and the circle symbols were also taken from Ref. [40] for experimental data.

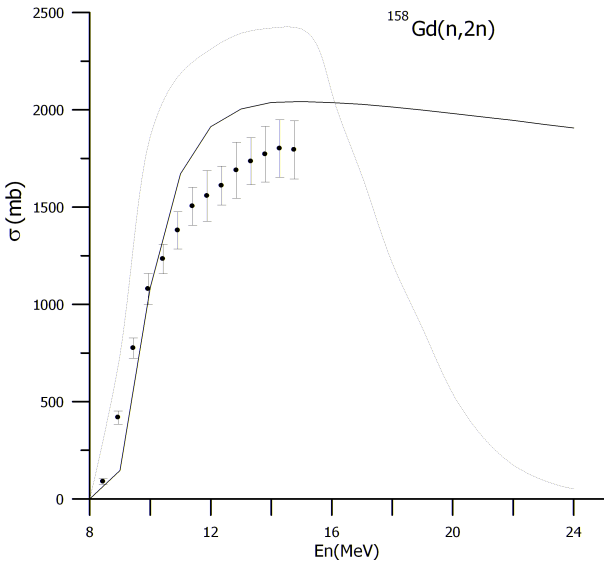

Fig. 7. The calculated and experimental (n,2n) cross-section for ^{158}Gd(n,2n). The solid curve is exciton model plus evaporation; the dashed curve is GDH model plus evaporation. The experimental data were taken from Ref.[39].

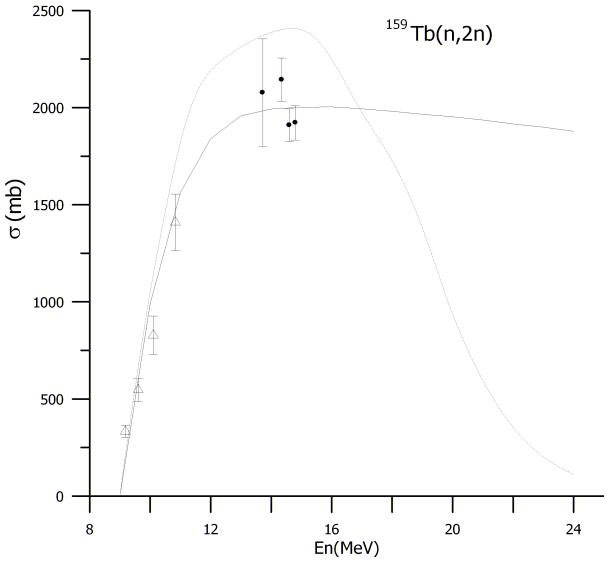

Fig. 8. The calculated and experimental (n,2n) cross-section for ^{159}Tb(n,2n). The solid curve is exciton model plus evaporation; the dashed curve is GDH model plus evaporation. The triangle symbols were taken from Ref. [42] and the circle symbols were also taken from Ref. [40] for experimental data.

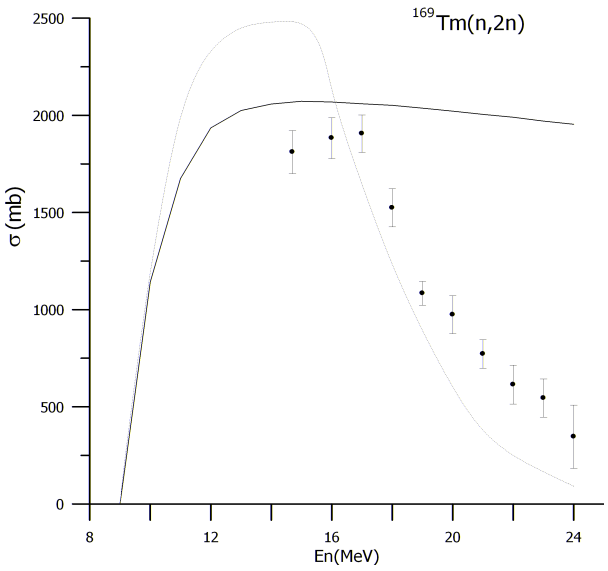

Fig. 9. The calculated and experimental (n,2n) cross-section for ^{169}Tm (n,2n). The solid curve is exciton model plus evaporation; the dashed curve is GDH model plus evaporation. The experimental data were taken from Ref. [43].

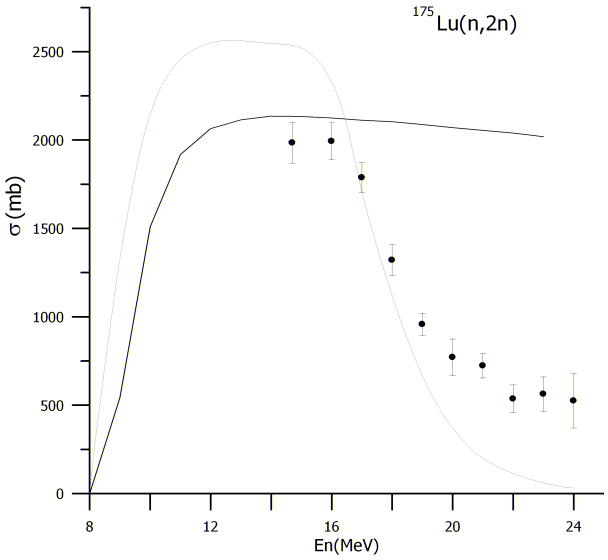

Fig. 10. The calculated and experimental (n,2n) cross-section for ^{175}Lu(n,2n). The solid curve is exciton model plus evaporation; the dashed curve is GDH model plus evaporation. The experimental data were taken from Ref. [43].

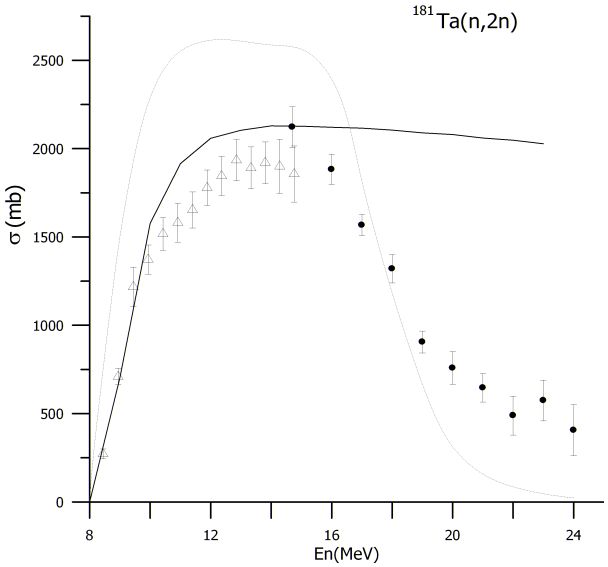

Fig. 11. The calculated and experimental (n,2n) cross-section for ^{181}Ta(n,2n). The solid curve is exciton model plus evaporation; the dashed curve is GDH model plus evaporation. The triangle symbols were taken from Ref. [32] and the circle symbols were also taken from Ref. [43] for experimental data.

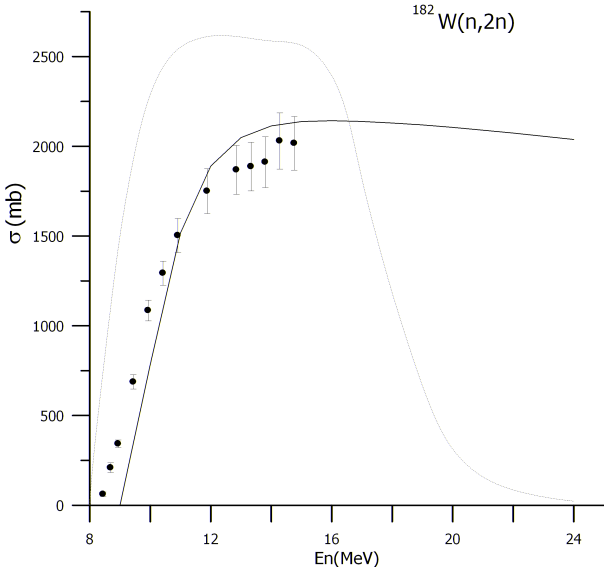

Fig. 12. The calculated and experimental (n,2n) cross-section for ^{182}W(n,2n). The solid curve is exciton model plus evaporation; the dashed curve is GDH model plus evaporation. The experimental data were taken from Ref. [39].

The Weisskopf-Ewing (WE) model was used in both models (exciton model and GDH model) for equilibrium calculation. The exciton model (PCROSS) code uses a master equation and treat equilibrium and pre-equilibrium in a "unified" way. The level density formula of Williams was used. The Hybrid model structure is very similar to the "never-come-back" approximation of the exciton model; however, different expressions for the mean lifetimes were used. In particular, the mean lifetime of the hybrid model refers to the particle under consideration and hence depends upon out going energy ε, whereas in the usual exciton model it is related to the nuclear system as a whole and is only function of n. This results in a different expression for the internal transition rate $\lambda_+(\varepsilon)$ that is derived from the concept of mean free path, rather than by a parametrization of the avarege transition matrix element $\langle M^2 \rangle$ and also in a different expression for the emission rate $\lambda_c(\varepsilon)$ occurring in the mean life time. The GDH model is made according to incoming orbital angular momentum l in order to account for the effects of the nuclear-density distribution. This leads to increased emission from the surface region of the nucleus, and thus to increased emission of high-energetic particles. The comparisons of these two models have been given in detail in Ref. [37].

We, therefore, reached the following conclusion: The (n,2n) cross-sections were calculated using other semi-empirical formulas for the incoming energies which satisfy the condition $U_{\mathrm{R}} = E_{\mathrm{n}} + Q_{\mathrm{n,2n}} = 6 \pm 1$ MeV. The obtained results were discussed and compared with the available experimental data. The exciton model for the incoming energies about 14–15 MeV is very successful for all the neighboring deformed nuclei in the region of rare-earth elements. The GDH model calculations for the same energies are higher than the experimental values for neighbor deformed nuclei. The GDH model is about 10–15% higher than exciton model in the region of $U_{\mathrm{R}} = E_{\mathrm{n}} + Q_{\mathrm{n,2n}} = 6 \pm 1$ MeV. However, GDH model is very successful than exciton model above the incident energy 15 MeV. In this study, these differences could be possible resulted from including the direct interactions of the exciton model. The PCROSS program code also included consideration of the direct excitation of low excitation energy levels in the calculation of (n, n') inelastic scattering spectra. Moreover, different initial exciton numbers have been used in these two models. Here the pairing energy and the mass shell correction were taken into consideration, and better results have been obtained. Especially in the region of $U_{\mathrm{R}} = 6 \pm 1$ MeV, the results obtained have been found to be well in agreement between the experimental data and the calculated values using Bychkov [28] formula, which linearly depends on the mass number A and the asymmetry parameter s.

References

[1] N. Bohr: *Nature* **137** (1936) 344 ; N. Bohr: *Science* **86** (1937) 161

[2] Ya.I. Frenkel: *Sov. Phys.* **9** (1936) 533

[3] J.J. Griffin: *Phys. Rev. Lett.* **17** (1966) 478

[4] H. Gruppelaar et al.: *Nuovo Cimento* **9** (1986) 1 ; H. Gruppelaar, M. Blann: *Annu. Rev. Nucl. Sci.* **25** (1975) 123

[5] E. Běták: *Comp. Phys. Com.* **9** (1975) 92-101

[6] H. Feshbach et al.: *Annu. Phys. (NY)* **125** (1980) 429

[7] T. Tamura et al.: *Phys. Rev. C* **26** (1982) 379

[8] H. Ahmadov et al.: *Nucl. Phys. A* **706** (2002) 313

[9] Ş. Okuducu, H. Ahmadov: *Phys. Lett. B* **565** (2003) 102

[10] V.F. Weisskopf, D.H. Ewing: *Phys. Rev.* **57** (1940) 472
[11] C.K. Cline, M. Blann: *Nucl. Phys. A* **172** (1971) 225
[12] C.K. Cline: *Nucl. Phys. A* **193** (1972) 417
[13] I. Ribansky et al.: *Nucl. Phys. A* **205** (1973) 545
[14] J.M. Akkermans et al.: *Phys. Rev. C* **22** (1980) 73
[15] C. Kalbach: *Z. Phys. A* **283** (1977) 401
[16] S.K. Gupta: *Z. Phys. A* **303** (1981) 329
[17] M. Baba, M. Ishikawa, N. Yabuta, T. Kikuchi, H. Wakabayashi, M. Mirakawa: *Int. Conf. "Nucl. Data for Science and Technology"* May-June 1988, Mito, Japan.
[18] A. Pavlik, H. Vonach: *Report IRK, "Evaluation of the angle integrated neutron emission cross-sections from the interaction of 14 MeV neutrons with medium and heavy nuclei"*, Vienna 1988
[19] R. Capote, V. Osorio, R. Lopez, E. Herrera, M. Piris: *Final report on Research contract 5472/RB, INDC(CUB)-004, Higher Institute of Nuclear Science and Technology*, Cuba, March 1991, (PCROSS program code)
[20] S. Raman et al.: *Atomic Data & Nuclear Data Tables* **36** (1987) 1
[21] C.M. Lederer, V.S. Shirley: *Table of Isotope* (1978)
[22] M. Blann, H.K. Vonach: *Phys. Rev. C* **28** (1983) 1475
[23] M. Blann et al.: *Nukleonika* **21** (1976) 335
[24] R. Hofstadter: *Annu. Rev. Nucl. Sci.* **7** (1957) 295
[25] E. Běták et al.: *Nucl. Sci. and Eng.* **132** (1999) 295
[26] E. Tel et al: *J. Phys. G: Nucl. Part. Phys.* **29** (2003) 2169
[27] C. Konno et al.: *JAERI-1329, Japan Atomic Energy Research Ins* (1993)
[28] V.M. Bychkov, V.N. Manokhin, A.B. Pashchenko, V.I. Plyaskin: *Handbook of cross-sections for neutron induced threshold reactions*, Energoizdat, Moscow (1982) (in Russian)
[29] S. Pearlstein: *Analysis of (n,2n) Cross-section for Nuclei of Mass* $A \geq 30$ *BNL-897.* Brookhaven National Laboratory (1964)
[30] A.H. Wapstra, K. Bos: *Atomic Data & Nuclear Data Tables* **19** (1977) 185
[31] M. Blann, J. Bisplinghoff: *"CODE ALICE/LIVERMORE 82"*. UCID-19614 (1982)
[32] F.C. Williams: *Nucl. Phys. A* **166** (1971) 231
[33] W. Dilg et al.: *Nucl. Phys. A* **217** (1973) 269
[34] D. Wilmore, P.E. Hodgson: *Nucl. Phys.* **55** (1964) 673
[35] F.D. Becchetti, G.W. Greenlees: *Phys. Rev.* **182** (1969) 1190
[36] J.R. Huizenga, G. Igo: *Nucl. Phys.* **29** (1962) 462
[37] C. Kalbach: *Acta Phys. Slov.* **25** (1975) 100
[38] An Jong Do et al.: *J. Phys. G: Nucl. Part. Phys.* **10** (1984) 91
[39] J. Frehaut, A. Bertin, R. Bois, J. Jary: *Status of (n,2n) cross-section measurements at Bruyeres–Le-Chatel.* (C,75KIEV,7506), Full paper of contribution to symposium on neutron cross-sections from 10-50 MeV, held at upton L.I. (U.S.A.) (1980), 12-14
[40] Y. Wang et al.: *J. High Energy Phys. and Nucl. Phys., Chinese ed.* **16** (1992) 731
[41] S.M. Qaim: *Nucl. Phys. A* **224** (1974) 319
[42] S.M. Qaim, F. Cserpak, J. Csikai: *Cross-sections of Eu-151(n,2n) and Tb-159(n,2n) Reactions Near Their Thresholds.* Int. J. Appl. Rad. Isot. (1993), (J,ARI,47,(5/6), 569,1996) Main Reference. Old Data Renormalized, New Ones Given (S,INDC(NDS)-342,47,199602) Corrected Data (W,QAIM,1993), submited to Int. J. Appl. Rad. Isot.
[43] L.R. Veeser et al.: *Phys. Rev. C* **16** (1977) 1792